Journal of Power Sources 180 (2008) 586–590

Contents lists available at ScienceDirect

Journal of Power Sources

journal homepage: www.elsevier.com/locate/jpowsour

Short communication

$LiBF_3Cl$ as an alternative salt for the electrolyte of Li-ion batteries

Sheng Shui Zhang*

U.S. Army Research Laboratory, AMSRD-ARL-SE-DC, Adelphi, MD 20783-1197, USA

ARTICLE INFO

Article history:
Received 23 January 2008
Received in revised form 12 February 2008
Accepted 13 February 2008
Available online 19 February 2008

Keywords:
$LiBF_3Cl$
$LiBF_4$
Electrolyte
Solid electrolyte interphase
Li-ion battery

ABSTRACT

$LiBF_3Cl$ was synthesized by reacting BF_3 etherate and LiCl in an organic media, and evaluated as a salt for the electrolyte of Li-ion batteries. XRD results showed that $LiBF_3Cl$ has the same crystallographic structure as $LiBF_4$ except for little difference in the lattice parameter. With a 3:7 (w/w) solvent blend of ethylene carbonate and ethyl methyl carbonate, $LiBF_3Cl$ electrolyte was found to have lower liquidus temperature than $LiBF_4$ analogue either due to its higher solubility or due to its higher tendency in forming a super-cooling solution, which was related to the less symmetry of BF_3Cl^- anion. Meanwhile, $LiBF_3Cl$ electrolyte displayed excellent ability in passivating Al at high potentials due to the similar chemical composition of $LiBF_3Cl$ and $LiBF_4$. Most importantly, the $LiBF_3Cl$ electrolyte was superior to the $LiBF_4$ electrolyte in facilitating the formation of solid electrolyte interphase (SEI) on graphite electrode, which not only increased Coulombic efficiencies of the SEI formation, but also prolonged cycle life of the Li-ion batteries. The merits above make $LiBF_3Cl$ very promising as an alternative lithium salt for the electrolyte of Li-ion batteries.

Published by Elsevier B.V.

1. Introduction

$LiBF_4$ has been known to be superior to $LiPF_6$ in providing better low temperature performance of Li-ion batteries [1–3]. The reason is because the batteries with $LiBF_4$ salt have lower charge-transfer resistance (R_{ct}), which has been identified as the major contribution to the overall impedance of a Li-ion battery at low temperatures [4,5]. Compared with $LiPF_6$, the main drawbacks of $LiBF_4$ are (1) inferior ability in assisting formation of solid electrolyte interphase (SEI) on the surface of graphite electrode [6,7], and (2) poor ability in forming a super-cooling solution of the electrolytes at low temperatures either because of its low solubility or because of freezing of the electrolytic solvents [2]. The former is due to that the BF_4^- anion is too stable to be participated in the SEI formation, and the latter is due to high symmetry and small size of the BF_4^- anion. Reduction in the stability and symmetry of the BF_4^- anion is assumed to alleviate the drawbacks of $LiBF_4$, which have restricted its application in the electrolyte of Li-ion batteries. This idea has been confirmed by our previous work [8], in which we synthesized a $LiBF_2(C_2O_4)$ salt and found that it combined the advantages of both $LiBF_4$ and $LiB(C_2O_4)_2$. Compared with $LiBF_4$, $LiBF_2(C_2O_4)$ was much superior in facilitating SEI formation and stabilizing SEI at high temperatures. Compared with $LiB(C_2O_4)_2$, $LiBF_2(C_2O_4)$ showed higher solubility in organic solvents and provided Li-ion batteries with much better low temperature performance and rate capability.

Encouraged by the results above, in this work we synthesized $LiBF_3Cl$ and evaluated it as an alternative salt for the electrolyte of Li-ion batteries. Due to the asymmetric structure of BF_3Cl^- anion, this new salt is expected to have higher solubility in organic solvents than $LiBF_4$. More importantly, the weaker coordination of Cl to boron central atom than F promotes the formation of BF_3 based on the chemical equilibrium of "$BF_3Cl^- \leftrightarrow BF_3 + Cl^-$", which is further participated in the SEI formation. In the present work, the essential properties of $LiBF_3Cl$ as an electrolytic salt of the Li-ion batteries will be evaluated and discussed. These properties include ionic conductivity of the electrolyte, the ability of electrolyte in passivating Al foil at high potentials, SEI formation on graphite electrode, and cycling performance of the Li-ion cells with the electrolyte consisting of $LiBF_3Cl$ salt.

2. Experimental

$LiBF_3Cl$ was synthesized by reacting BF_3 and LiCl as a procedure described below [9]. In a glove-box having moisture level less than 20 ppm, 4.26 g (0.03 mol) of BF_3 etherate was diluted with 20 mL of dimethoxyethane and placed in a Teflon reactor, to which 1.27 g (0.03 mol) of dried LiCl was added with stirring. By adding small amount of methanol as a reaction aid, numerous bubbles (diethyl ether) immediately came out from the surface of LiCl, and the solid LiCl started to dissolve slowly. The mixture was stirred for 16 h at 40 °C, which left very small amount of LiCl insoluble. The resided LiCl was filtered out and the resulting filtrate was concentrated under reduced pressure until white product was obtained. The crude product was purified via re-crystallization and dried at

* Tel.: +1 301 394 0981; fax: +1 301 394 0273.
E-mail address: szhang@arl.army.mil.

0378-7753/$ – see front matter. Published by Elsevier B.V.
doi:10.1016/j.jpowsour.2008.02.018

100–110 °C under vacuum for 8 h, which gave 2.61 g of $LiBF_3Cl$ white powder (yield = 79%, based on the weight of LiCl). Crystallographic structure of the salt was characterized by X-ray diffraction (XRD) using a Philips PW 1840 X-ray diffractometer with Cu Kα radiation. To protect the salt from moisture in the course of measurement, an X-ray inactive polyimide film was covered over the sample cell. NMR spectroscopes of $LiBF_3Cl$ were analyzed using d^6-acetone as the solvent, giving the chemical shifts below:

- ^{19}F-NMR: 156.05 ppm vs. 152.63 ppm of $LiBF_4$ (referenced to Freon-12);
- ^{11}B-NMR: 0.85 ppm vs. 1.24 ppm of $LiBF_4$ (referenced to H_3BO_3).

In the same glove-box used above, a 3:7 (w/w) blend of ethylene carbonate (EC) and ethylmethyl carbonate (EMC) was prepared as the electrolytic solvent to evaluate the electrochemical properties of $LiBF_3Cl$, in which both solvents were in battery electrolyte grade and purchased from Ferro Corporation. Using the solvent blend made above, a 1 m (molality) $LiBF_3Cl$ and a 1 m $LiBF_4$ electrolyte were prepared, respectively. Ionic conductivity of the electrolyte was determined from the impedance of the solution measured using a two-platinum-electrode cell. Chemical compatibility of the electrolyte and metal Li was evaluated by monitoring impedance change of a three-electrode button cell, in which three pieces of Li foils were used as the working, reference and counter electrodes, respectively. Detailed description about the cell structure and assembly was introduced in previous papers [10,11]. The impedance was potentiostatically measured at the open-circuit potential using a Solartron SI 1287 Electrochemical Interface and a SI 1260 Impedance/Gain-Phase Analyzer with an ac oscillation of 10 mV amplitude over the frequencies from100 kHz to 0.01 Hz, and the obtained spectra were analyzed using ZView software.

An EG&G PAR Potentiostat/Galvanostat Model 273A was used to examine electrochemical properties of the electrolyte. To determine the electrochemical stability window of the electrolyte, a newly scratched Cu and Al wire, respectively, with a diameter of 1.0 mm was used as the working electrode by exposing a 1 cm length of wire to the electrolytic solution, and lithium foils were used as the counter and reference electrodes. The *I–V* response of the first two sweeps was recorded at a potential scanning rate of 5 mV s^{-1}. For evaluation of the cell performance of the electrolyte, standard electrode films of graphite coated on a Cu foil and $LiNi_{0.8}Co_{0.15}Al_{0.05}O_2$ (NCA) coated on an Al foil were used to assemble button cells in which a Celgard® 2500 membrane was used as the separator and 0.15 mL electrolyte was filled. Composition of the electrodes was 90% NCA (6–8 μm, Mitsubishi)/2.5% KS-6 graphite/2.5% Super P carbon/5% PVDF, and 90% MCMB 25–28 (40 μm, Osaka Gas Chem.)/3% Super P carbon/7% PVDF (all in wt.%), respectively. The cells were cycled on a Maccor Series 4000 tester at room temperature under the conditions as described in the figure caption of each.

3. Results and discussion

3.1. Crystallographic structure of $LiBF_3Cl$

Crystallographic structure of $LiBF_3Cl$ was analyzed by comparing XRD patterns of $LiBF_3Cl$ and $LiBF_4$ as indicated in Fig. 1. It is shown that these two salts have very similar diffraction peaks and relative intensity, suggesting the same crystallographic structure. A little difference is that the diffraction peaks of $LiBF_3Cl$ were shifted toward slightly lower and peaks at 18.5° and 22.0° were disappeared, as compared to those of $LiBF_4$. This phenomenon could be attributed to the less symmetric structure of BF_3Cl^- anion due to the substitution of chloride for one fluoride in $LiBF_4$. The lower diffraction angles reflect the fact that $LiBF_3Cl$ has slightly larger cell lattice parameters than $LiBF_4$ crystals.

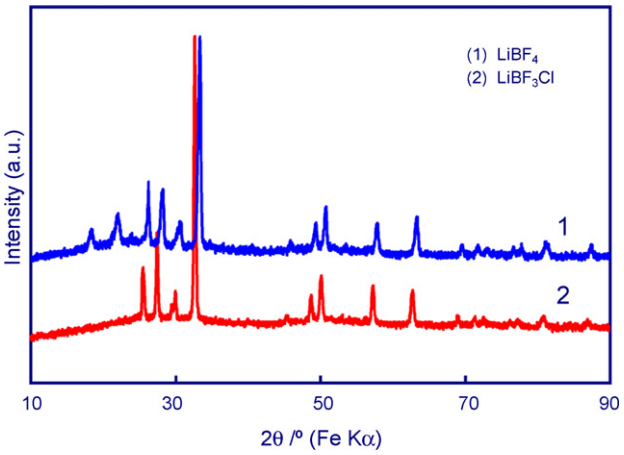

Fig. 1. XRD patterns of $LiBF_3Cl$ and $LiBF_4$.

3.2. Ionic conductivity and electrochemical window of $LiBF_3Cl$ electrolyte

Ionic conductivities of $LiBF_4$ and $LiBF_3Cl$ solutions in a 3:7 (w/w) EC/EMC solvent blend are compared in Fig. 2. Above −50 °C, the $LiBF_3Cl$ solution exhibits very little higher conductivity due probably to the less symmetry and larger size of BF_3Cl^- anion which are known to increase dissociation of the ions. At −60 °C, the conductivity of $LiBF_4$ solution is suddenly dropped while that of $LiBF_3Cl$ solution remains a normal decreasing trend. The similar behavior has been observed from a 1:1:1 (w/w) EC/PC/EMC system [2], and it is due to phase changes of the electrolyte caused either by $LiBF_4$ precipitation or by solvents freezing. Inside the battery, such phase transitions may occur at much higher temperatures since the particles of electrode components serve as the crystallizing seeds [12]. The results above verify that $LiBF_3Cl$ is superior to $LiBF_4$ in promoting the formation of a super-cooling solution, which can be attributed to the asymmetric structure and large size of the BF_3Cl^- anion.

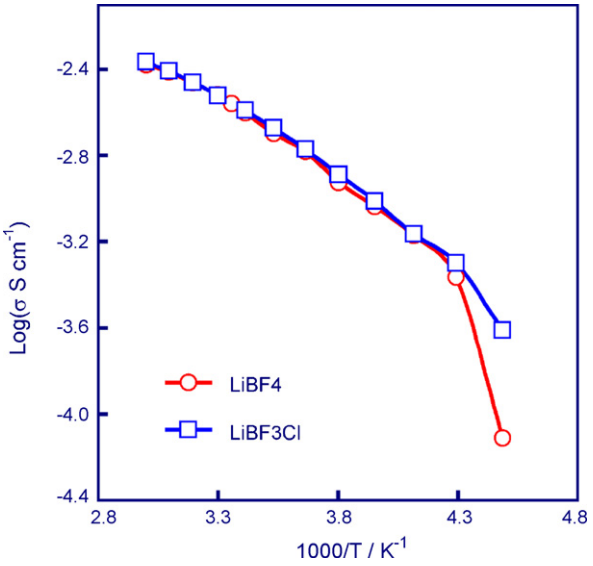

Fig. 2. Arrhenious plots of the ionic conductivities of 1.0 m lithium salt in a 3:7 (w/w) EC/EMC solvent blend.

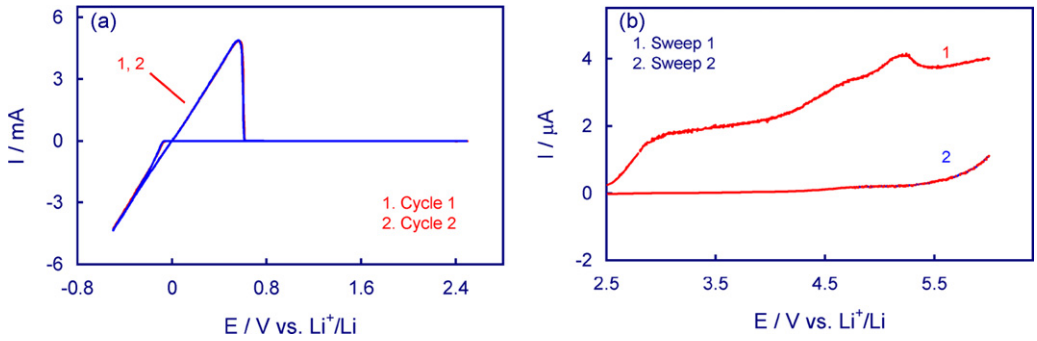

Fig. 3. Electrochemical window of a 1.0 m $LiBF_3Cl$ 3:7 EC/EMC electrolyte, which was measured by using a newly scratched Cu and Al wire, respectively, as the working electrode. (a) Cu wire; (b) Al wire.

Fig. 3 displays electrochemical window of the $LiBF_3Cl$ electrolyte against Cu (cathodic) and Al (anodic), respectively. On the cathodic side, the stability of the electrolyte is limited by the potentials of plating and stripping of metal Li (Fig. 3a). In particular, cyclic voltammograms of the first and second cycles are in a completely overlapped pattern, indicating excellent cycleability of metal Li in the $LiBF_3Cl$ electrolyte. This feature is of great importance in both rechargeable Li and Li-ion batteries. On the anodic side, Al is electrochemically passivated very well in the course of the first sweep, as indicated by the current increasing nearly from the open-circuit potential and being suppressed at higher potentials. In the second sweep, the anodic current is remained at the ground level until 5.5 V vs. Li^+/Li (Fig. 3b) at which the electrolytic solvents start to be oxidized. This observation indicates that with $LiBF_3Cl$ as the solute of an electrolyte, both Al and solvents are stable up to 5.5 V. In previous works [13,14], it has been shown that the corrosion behavior of Al was mainly affected by the anion of the electrolytic salt, instead of the solvents. The excellent stability of Al observed here is attributed to the incorporation of $LiBF_3Cl^-$ anion in forming a protective surface layer. The merits above make $LiBF_3Cl$ well qualified for an alternative electrolytic salt of the Li-ion batteries.

3.3. Chemical compatibility of $LiBF_3Cl$ electrolyte and metal Li

Stability of metal Li against $LiBF_3Cl$ electrolyte was evaluated by monitoring impedance change of metal Li. In order to accelerate the reactions of Li and electrolyte components, the cell was placed in a 60 °C oven. As shown in Fig. 4a, the typical impedance spectrum consists of two partially overlapped semicircles sandwiched by two inductive loops at high frequency end and at low frequency end, respectively. The inductive loop at high frequencies is common in Li-ion batteries [15,16], and it is related to many factors including cell configuration, cell holder, and even the settings of the frequency analyzer. The reason for the inductive loop at low frequencies is not clear, however, such loops have been frequently observed in the case of metal corrosion in aqueous solutions. Many authors attributed such a loop to the relaxation of surface species accompanying with the dissolution of metal [17,18], and in the present case this inductive loop could be related to a similar process reflecting the reversible dissolution (reaction) of "$Li–e \leftrightarrow Li^+$" on the surface of metal Li.

In the present work, special interest was placed in two semicircles in medium frequency regions, of which the one at higher frequencies relates to the impedance of passivation layer (or called solid electrolyte interphase) and the other one at lower frequencies relates to charge-transfer process on the electrolyte-Li interface. Based on the model described previously [19,20], the passivation layer resistance (R_{sei}) and charge-transfer resistance (R_{ct}) were fit using Zview software and plotted in Fig. 4b as a function of the storage time. It is shown that both resistances were increased rapidly in the initial period (~25 h), which is attributed to the formation and growth of passivation layer. After this period, the R_{sei} and R_{ct} became stable and their values were in comparable levels. These results verify that the $LiBF_3Cl$ electrolyte is quite compatible with metal Li that is often formed on the surface of graphite anode when a Li-ion battery is charged at high current rate or charged at low temperatures.

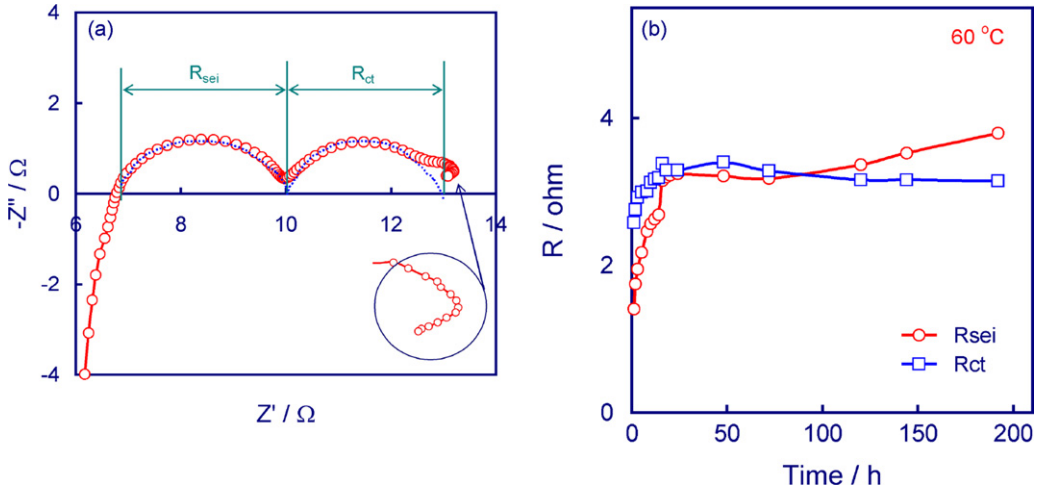

Fig. 4. Results of the impedance measurements on a three-electrode Li/Li/Li button cell with a 1.0 m $LiBF_3Cl$ 3:7 EC/EMC electrolyte. Working electrode was a metal Li disk with a diameter of 0.5 in., and the measurements were conducted at 60 °C. (a) A typical impedance spectrum and (b) time dependence of the resistances.

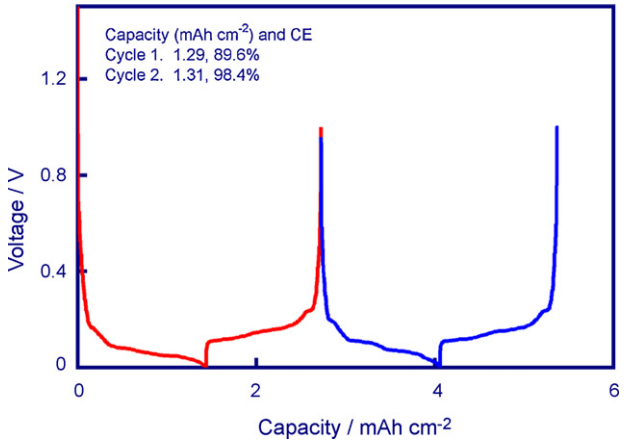

Fig. 5. Forming cycles of a Li/graphite half-cell, in which the cell was cycled at 0.1 C between 0.002 V and 1.0 V by starting discharge from the open-circuit voltage.

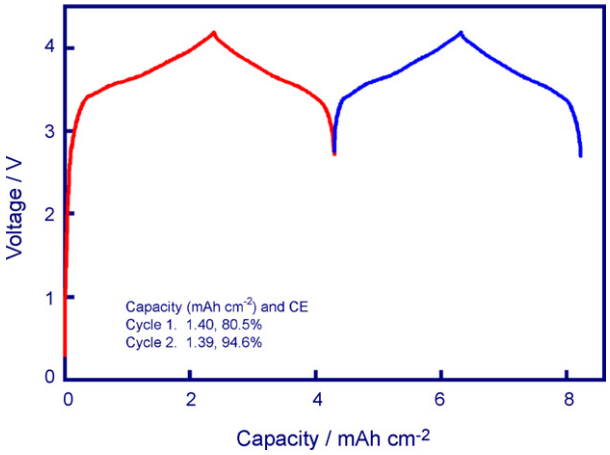

Fig. 7. Voltage profiles of the forming cycles of a graphite/$LiNi_{0.8}Co_{0.15}Al_{0.05}O_2$ Li-ion cell, which was recorded by cycling the cell at 0.1 C between 2.5 V and 4.2 V.

3.4. Characteristics of SEI formation in $LiBF_3Cl$ electrolyte

The characteristics of SEI formation on the surface of graphite anode and NCA cathode in the $LiBF_3Cl$ electrolyte were examined respectively using Li half-cells. The voltage profiles of the SEI formation of graphite in the first two cycles are shown in Fig. 5, from which Coulombic efficiency was estimated to be 89.6% and 98.4% for the first cycle and second cycle, respectively. These values are in the same level as those obtained in a 1.0 m $LiPF_6$ 3:7 EC/EMC [6]. On contrast, the efficiency of the first cycle for the same graphite electrode only could achieve 82% in a 1.0 m $LiBF_4$ 3:7 EC/EMC electrolyte [6]. The higher efficiency of the first cycle in $LiBF_3Cl$ electrolyte can be attributed to the relatively weak coordination of Cl with boron atom in the BF_3Cl^- anion, which promotes the anion splitting into pieces and combining into SEI components.

The characteristic of forming cycles of a Li/NCA half-cell is shown in Fig. 6. Coulombic efficiency of the first two cycles was determined to be 85.1% and 99.7%, respectively. These values are typical for the $LiNi_{1-x}M_xO_2$ family cathode materials. Two origins have been known to result in the initial irreversible capacities of such cathodes [21], including (1) irreversible change in crystallographic structure of the cathode due to Li^+ ions collapsing irreversibly into the sites of Ni^{2+} ions, and (2) limited oxidization of the electrolytic solvents on the surface of cathode. The former depends on chemical composition of the cathodes such as the value of x and the type of M, and usually increasing x value reduces the initial irreversibility. The latter is affected solely by the solvents instead of salt unless the salt is instable in the operating potential range, and this part of irreversible capacities are related to the formation of surface layer (or called solid electrolyte interphase) on the surface of active cathode materials.

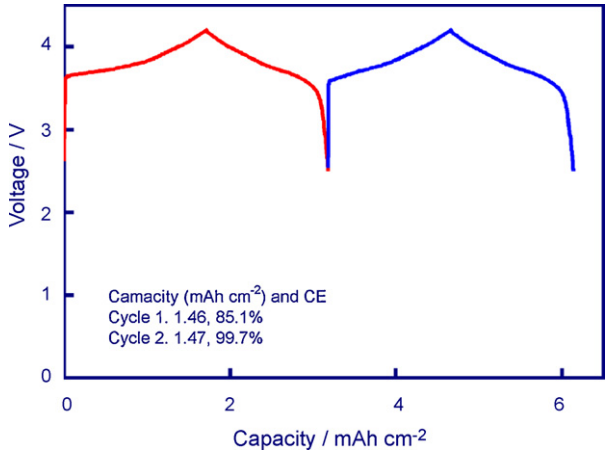

Fig. 6. Forming cycles of a Li/$LiNi_{0.8}Co_{0.15}Al_{0.05}O_2$ half-cell, in which the cell was cycled at 0.1 C between 2.5 V and 4.2 V by starting charge from the open-circuit voltage.

3.5. Cycling performance of Li-ion cells with $LiBF_3Cl$ electrolyte

Fig. 7 exhibits voltage profile of the initial two forming cycles for a graphite/NCA Li-ion cell, which shows a Coulombic efficiency of 80.5% and 94.6% for the first and second cycle, respectively. The efficiencies of the Li-ion cell appear to be lower than those of the individual half-cells, as discussed above. The reason is probably because capacities of the graphite and cathode were not in proper balance. Comparing the reversible capacities of half-cells as shown in Figs. 5 and 6, one finds that the cathode was overloaded. In this case, extra Li^+ ions from the cathode could result in the plating of metal Li on the graphite, which as a result led to lower efficiency of the Li-ion cell due to the known poor cycleability of metal Li. It should be pointed out that this is not the case in Li/graphite and Li/cathode half-cells since metal Li serves as a sufficient Li source.

After two forming cycles at low current (0.1 C), the cell was progressively cycled by raising the current to 0.5 C and lowering the upper limiting voltage to 4.1 V. Fig. 8 shows capacity retentions of

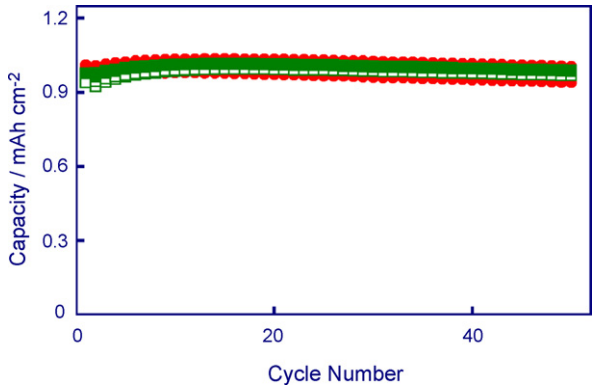

Fig. 8. Cycling performance of five identical Li-ion cells cycled at 0.5 C between 2.5 V and 4.1 V. Note that for the charging process, a taper charging at 4.1 V was followed until the current declined to 0.1 C as soon as voltage of the cell reached 4.1 V.

five identical cells as a function of cycle number. Due to lower upper limiting voltage, less Li^+ ions are available from the cathode. Thus, platting of metal Li on the graphite anode was effectively alleviated, which therefore enhances cycling efficiency of the cells. It can be seen in Fig. 8 that all five Li-ion cells maintained excellent capacity retention against the prolonged cycling. The results above reveal that $LiBF_3Cl$ is suitable for a solute of the electrolyte of the Li-ion batteries.

Finally, it should be mentioned that in addition to Li salt, a variety of tetra-alkyl ammoniums of the BF_3Cl^- anion can be synthesized simply by replacing LiCl with a corresponding ammonium chloride in the synthesis procedure described in experimental. The BF_3Cl^--based ammoniums are expected to be superior to the BF_4^- analogues for the applications in the electrolytes of double-layer capacitors, especially for low temperature electrolytes since the less symmetry of the BF_3Cl^- anion than BF_4^- anion favors increasing the dissociation and solubility of the ammonium in organic solvents. Furthermore, the less symmetric anion has been reported to be favorable for the formation of low melting point ionic liquids [22].

4. Conclusions

$LiBF_3Cl$ can be easily synthesized by reacting BF_3 and LiCl. It is shown that $LiBF_3Cl$ has excellent ability in passivating Al at high potentials due to its similar chemical composition as $LiBF_4$. Attributing to the less symmetry of BF_3Cl^- anion, $LiBF_3Cl$ has higher solubility than $LiBF_4$ and is superior to $LiBF_4$ in promoting the formation of a super-cooling solution of the electrolyte. More importantly, $LiBF_3Cl$ is more efficient in facilitating the SEI formation of graphite electrode. These merits make $LiBF_3Cl$ very promising as a salt for the electrolyte of Li-ion batteries. Furthermore, its tetra-alkyl ammonium analogues are expected to have extensive applications in the electrolyte of double-layer capacitors, especially for the applications at low temperatures.

Acknowledgments

The author thanks Dr. Jeff Wolfenstein for his assistance in XRD measurement of the moisture sensitive materials and Dr. Kang Xu for his assistance in NMR analysis.

References

[1] S.S. Zhang, K. Xu, T.R. Jow, Electrochem. Commun. 4 (2001) 928.
[2] S.S. Zhang, K. Xu, T.R. Jow, J. Solid State Electrochem. 7 (2003) 147.
[3] S.S. Zhang, K. Xu, T.R. Jow, 205th ECS Meeting Abstracts, San Antonio, TX, May 9–14, 2004, p. 82.
[4] S.S. Zhang, K. Xu, T.R. Jow, J. Power Sources 115 (2003) 137.
[5] S.S. Zhang, K. Xu, T.R. Jow, Electrochim. Acta 49 (2004) 1057.
[6] S.S. Zhang, K. Xu, T.R. Jow, J. Electrochem. Soc. 149 (2002) A586.
[7] S.S. Zhang, K. Xu, J.L. Allen, T.R. Jow, J. Power Sources 110 (2002) 216.
[8] S.S. Zhang, Electrochem. Commun. 8 (2006) 1423.
[9] S.S. Zhang, K. Xu, T.R. Jow, U.S. Patent Application, ARL Docket #05-33, 2005.
[10] S.S. Zhang, J. Power Sources 163 (2007) 713.
[11] S.S. Zhang, J. Power Sources 163 (2006) 567.
[12] S.P. Ding, K. Xu, S.S. Zhang, T.R. Jow, K. Amine, G.L. Henriksen, J. Electrochem. Soc. 146 (1999) 3974.
[13] S.S. Zhang, T.R. Jow, J. Power Sources 109 (2002) 458.
[14] S.S. Zhang, J. Power Sources 162 (2006) 1379.
[15] G. Nagasubramanian, J. Power Sources 87 (2000) 226.
[16] S.S. Zhang, K. Xu, T.R. Jow, J. Power Sources 160 (2006) 1403.
[17] S.E. Frers, M.M. Stefenel, C. Mayer, T. Chierchie, J. Appl. Electrochem. 20 (1990) 996.
[18] M. Metikos-Hukovic, R. Babic, Z. Grubac, J. Appl. Electrochem. 32 (2002) 35.
[19] S.S. Zhang, M.H. Ervin, D.L. Foster, K. Xu, T.R. Jow, Proceedings of the 41st Power Sources Conference, Philadelphia, PA, June 14–17, 2004, pp. 105–108.
[20] S.S. Zhang, M.H. Ervin, D.L. Foster, K. Xu, T.R. Jow, J. Solid State Electrochem. 9 (2005) 77.
[21] S.S. Zhang, K. Xu, T.R. Jow, Electrochem. Solid-State Lett. 5 (2002) A92.
[22] T. Herzig, C. Schreiner, D. Gerhard, P. Wasserscheid, H.J. Hores, J. Fluorine Chem. 128 (2007) 612.